Synthesis and Cylinder Microdomain Structures of Hybrid Block Copolymers of π-Conjugated and Dendritic Poly(phenylazomethine)s and Flexible and Linear PEO

Yang Gao, Xiwen Zhang, Miao Yang, Xinjun Zhang, and Wei Wang*

The Key Laboratory of Functional Polymer Materials and Institute of Polymer Chemistry, College of Chemistry, Nankai University, Tianjin 300071, China

Gerhard Wegner*

Max-Planck-Institute for Polymer Research, Ackermannweg 10, Postfach 3148, D-55128, Mainz, Germany

Christian Burger

Chemistry Department, Stony Brook University, Stony Brook, New York 11794-3400

Received December 17, 2006
Revised Manuscript Received January 26, 2007

Introduction

Most diblock copolymers, which have been widely studied, are composed of two different linear polymer chains joined together via covalent bonds. It has been demonstrated that linear−linear diblock copolymers can form a wide range of supramolecular structures from spheres and cylinders over bicontinuous morphologies to lamellae via a microphase separation in the melt.[1] It is well-known that the most important parameters controlling the structure formation are the volume fraction of two blocks, f_v, the Flory−Huggins segmental interaction parameter, χ, and the degree of polymerization, N. When one of the blocks becomes rigid, rod−coil block copolymers with conformational asymmetry are constructed and an additional orientational parameter is induced.[2] The strong tendency of the rigid block holding ordered packing structures results in the microphase separation occurring at relatively low molecular weights in comparison with flexible block copolymers.

Well-defined architectures of monodendrons and dendrimers can self-assemble into spherical or cylindrical supramolecular objects, which can further self-organize into giant crystals.[3] These studies gives us an opportunity to have an in-depth understanding of the correlation between the molecular architectures and supramolecular structures via self-organization. Hybrid block copolymers are synthesized by chemically combining a dendritic block with a linear block.[4] Such a large difference in the molecular architecture of the two blocks has attracted great attention. Theoretical and experimental studies have targeted to explore the effect of special architectures of dendritic blocks on the microdomain structure.[5,6] A theoretical review concerning the impact of the molecular asymmetry, arisen entirely from their architecture, on the different packings in block copolymer melts has been released recently.[6] It has been found that the unique shape of the dendritic blocks can manipulate the curvature of the boundary between microdomains, causing a boundary shift toward lower volume fractions. Furthermore, the increased asymmetry enhances the stability of those phases where the stiffer domains are on the "outside" of curved interfaces.

In this work we report our findings of microdomain structures of two hybrid diblock copolymers composed of rigid and dendritic blocks and flexible and linear blocks. Our goal is to understand the influence of the differences in architecture and rigidity between two blocks on the microdomain structure. The rigid blocks are second- and third-generation poly(phenylazomethine) (DPA) dendrons containing π-conjugated backbones which confer a 2D conformational rigidity and persistent molecular shape into block copolymers, while the flexible block is a hydrophilic poly(ethylene oxide) (PEO) having a molecular weight of $\bar{M}_n = 2000$ g/mol to impart coil conformation and hydrophilicity into the block copolymers. We will concern the influence of the confirmatory molecular shape of the dendritic DPA blocks on boundary curvature between two blocks.

Results and Discussion

Synthesis. The preparation of the hybrid block copolymers is summarized in Scheme 1. Boronic ester-terminated PEO **A** was prepared from etherification of the monohydroxy-PEO with an excess amount of 4-boronic ester benzoic acid. The targeted DPA dendrons have one iodic function at the focal point of the second (**B2-2**) and third generation (**B3-2**). Aryl iodide was chosen as anchor group because it easily undergoes a Suzuki cross-coupling (SCC) reaction in high yield, even in situations where considerable steric congestion can be expected in the focus of dendrons.[7]

The synthetic sequence started from hexyl-modified aromatic building blocks **B1**, which was obtained via the standard Williamson etherification by 4,4′-diphenyl ketone and 1-hexyl bromide. Reaction of **B1** and **B2-1** with 4,4′-diamine benzophenone by the convergent method[8] gives the corresponding periphery-modified dendrons G2 (**B2-1**) and G3 (**B3-1**) with ketones at the focal point. The dehydration reactions of **B2-1** and **B3-1** with 4-iodoaniline converted these aromatic ketones into the corresponding aryl iodides **B2-2** and **B3-2**.

The block copolymers **A-B2** and **A-B3** were prepared by the Suzuki cross-coupling reaction of boronic ester-terminated PEO **A** with DPA dendrons **B2-2** and **B3-2**, respectively. The structures and purity of the block copolymers were checked by NMR spectroscopy and matrix-assisted laser desorption ionization time-of-flight (MALDI-TOF). The 400 MHz ^{1}H NMR spectra indicates purity higher than 98%, and the mass spectra exclude any indication of side products. Especially, there are no signals for nonreacted PEO chains.

Molecular Weight and Distribution. Figure 1 shows the absolute molecular weight and molecular weight distributions of block copolymers and pure PEO determined using MALDI-TOF. The molecular weight distribution can be assumed to be Gaussian. Table 1 lists the number-average molecular weight, $\bar{M}_n$, and the polydispersity index (PDI), $\bar{M}_w/\bar{M}_n$, of the three samples. Note that $\bar{M}_n = 3055$ g/mol for **A-B2** and $\bar{M}_n = 4222$ g/mol for **A-B3**, and $\bar{M}_w/\bar{M}_n$ is very close to one, meaning a narrow distribution of our samples.

The volume fractions of the PEO block, f_v, are also listed in Table 1. Densities of PEO were available from the literature.[9] The molecular densities of **A-B2** and **A-B3** were obtained by two ways: volume increment prediction of density[10] and a simple volume-extraction experiments (see Supporting Informa-

* Corresponding authors. E-mail weiwang@nankai.edu.cn or wegner@mpip-mainz.mpg.de.

10.1021/ma062881l CCC: $37.00
Published on Web 03/01/2007

Scheme 1. Synthesis Route

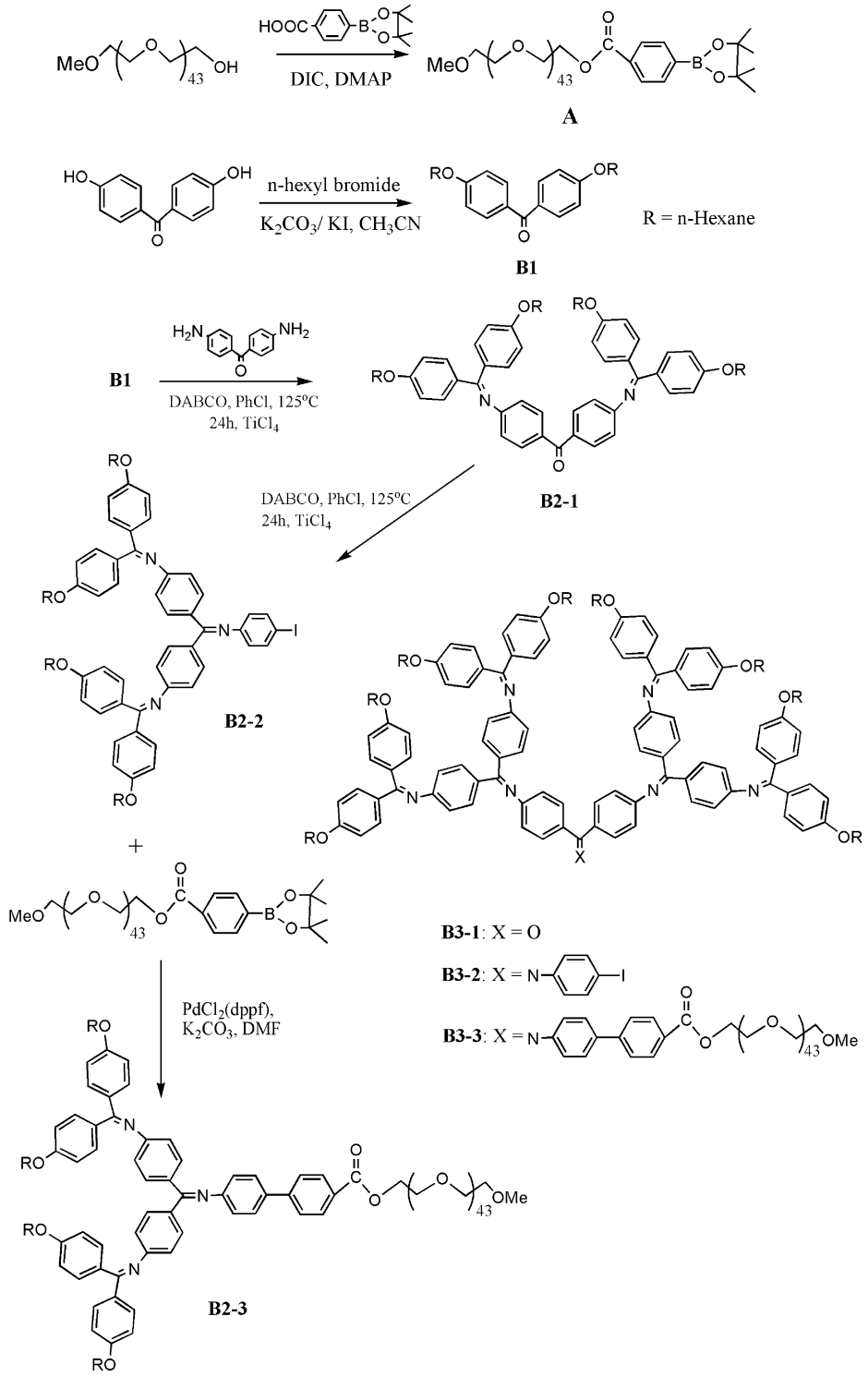

tion). The densities obtained from calculation and experiment matched consistently. The volume fractions of the PEO blocks in both **A-B2** and **A-B3** can be estimated by the molecular weights and the densities of both the individual PEO chain and the entire block copolymers, respectively.

Molecular Architecture and Properties. To date, several hybrid block copolymers composed of linear and dendritic blocks have been reported, which can self-organize into ordered aggregates.[5] Poly(benzyl ether) (PBE), poly(propyleneimine) (PII), poly(amidoamine) (PAMAM), polycarbosilane, and poly(benzyl ester) monodendrons have been used as the dendritic building blocks. These dendrons are relatively flexible and consequently tend to exhibit many conformations possibly including backfolding of the terminal monomers into the core.[11] Compared to the relatively flexible backbones of these dendrons, DPAs have a rigid π-conjugated framework, which imparts relatively fixed conformation as a wedge-shaped architecture (see Scheme S1 in Supporting Information).[13] This stiff architecture is a key property for finely controlled self-assembly behavior of DPAs and helped to understand the detailed self-assembling process. This can provide us with information about the molecular design strategy for novel self-assembling materials. In our system, the rigid characteristic of DPA monodendrons is obvious when compared with the focal PEO chains (see

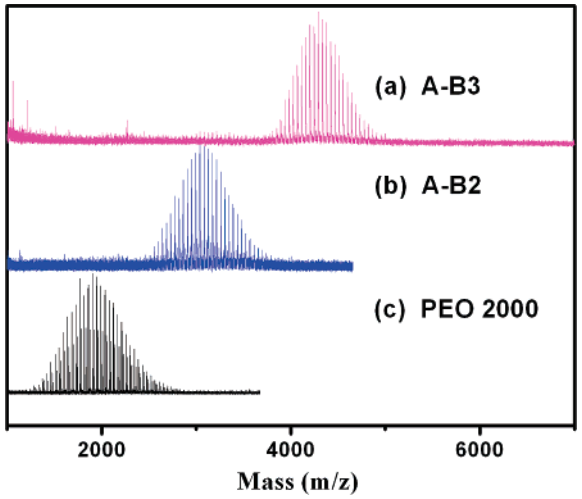

Figure 1. Molecular weight and its distribution of (a) **A-B3**, (b) **A-B2**, and (c) PEO 2000 samples determined by MALDI-TOF mass spectrometry.

Table 1. Basic Compound Parameters of the Samples Used

	$^{-}M_n$ (g/mol)				
	calcd	exp[a]	PDI	ρ (g/cm^3)	f_v[c] (%)
PEO 2000		1926	1.08	1.125−1.228[b]	100
A-B2	3079 (+Na^+)	3079	1.03	1.116[e]−1.178[d]	60.0−62.1
A-B3	4300 (+K^+)	4307	1.01	1.088[e]−1.117[d]	40.7−43.2

[a] Determined by MALDI-TOF spectrometer. [b] The density of amorphous and integrated crystal of PEO chains.[9] [c] The volume fraction of PEO blocks. [d] From calculation according to the literature.[11] [e] From our experiment.[10]

Scheme 2) and is expected to have a 2-dimensional structure with inherent curvature, which is unique for the rigid-linear diblock copolymers. Besides, the hexane modification of the dendrons further increases the dissimilarity in polarity between the dendritic and linear blocks.

Microdomain Structure Characterization by SAXS. Figure 2 shows SAXS profiles of PEO2000, **A-B2**, and **A-B3** block copolymers. The Bragg spacings of the scattering maxima are indicated in the figure. In all cases, two relatively broad peaks are observed. Thus, an unambiguous structure determination is

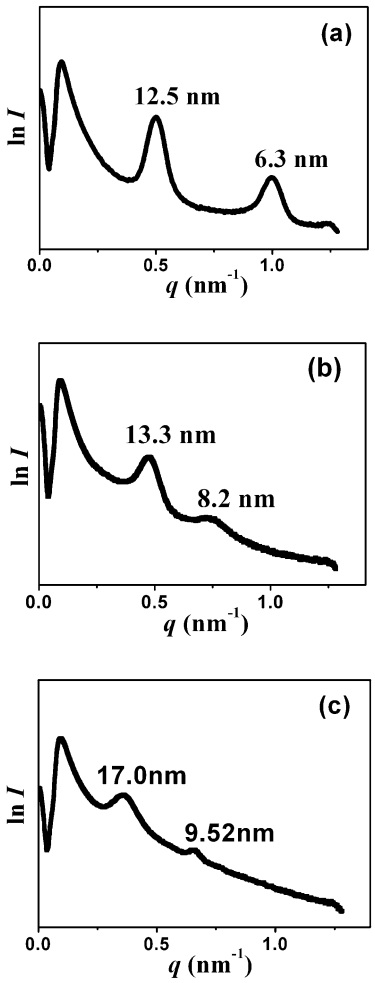

Figure 2. SAXS plots of (a) PEO 2000, (b) **A-B2**, and (c) **A-B3**.

Scheme 2. Molecular Architecture of the Block Copolymers

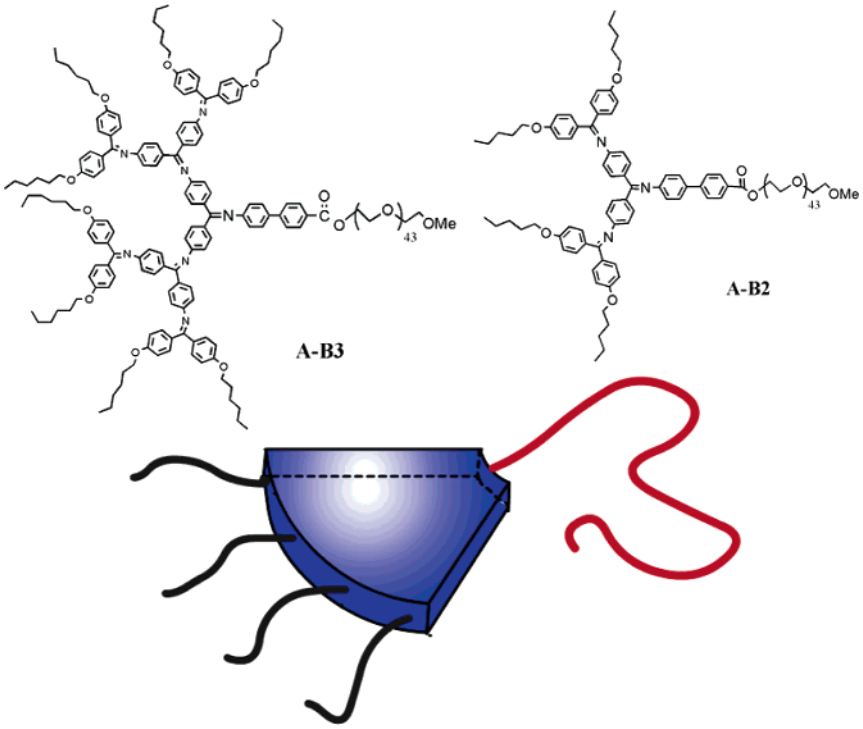

Table 2. X-ray Diffraction Data for A-B2 and A-B3

	lattice	lattice spacing/nm	*d*-spacing/nm obsd (calcd)	Miller indices	V_M[a] (nm^3)	V'_M[b] (nm^3)	V_{cell}[c] (nm^3)	*N* μ^d	*N* μ'	*N* μ_{av}
A-B2	*P*2	$a = 14.7$	13.3 (14.3,13.7,12.3)	(01,10, $1\bar{1}$)	3.7	4.7	156.3	27	21	24
		$b = 15.3$	8.2 (8.5)	(11)						
		$\gamma = 111°$								
A-B3	*P*6*mm*	$a = 19.6$	17.0 (16.9)	(10)	4.6	6.8	98.7	34	23	28
		$\gamma = 120°$	9.5 (9.8)	(11)						

[a] Calculated by density based on volume increment. [b] Calculated by density obtained from experiment. [c] Assuming the height of unit cell as 0.47 nm.[12] [d] μ represents the number of molecules within an elementary section of each column by $N = V_M/V_{cell}$, the height of the unit cell was assuming as 0.47 nm.

Scheme 3. Microdomain Structure of (a) A-B2 and (b) A-B3

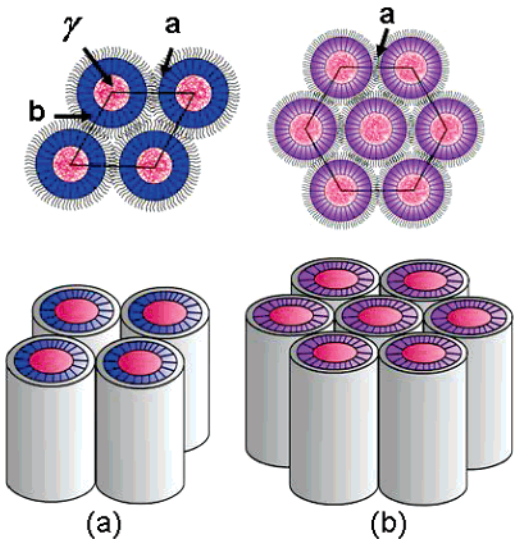

not possible, and we will resort to structure proposals having the highest simplicity and the least number of assumptions. The ratio of the two spacings is 2 for PEO2000, clearly indicative of a lamellar structure.

Block copolymer **A-B3** displays a diffraction pattern with two peaks at $q = 0.36$ and 0.66 nm^{-1} having a peak position ratio of close to $\sqrt{3}$, suggesting the presence of a two-dimensional hexagonal lattice (Figure 2c) with plane group *P*6*mm*. These are characteristics of the hexagonal columnar (Col_h) phase, corresponding to Miller indices (10) and (11), respectively. This reflection pattern corresponds to a 19.6 nm intercolumnar distance (a parameter of the hexagonal lattice). The number of **A-B3** molecules in the hexagonal unit cell was calculated as 28 molecules per unit cell for **A-B3** according to $N = V_M/V_{cell}$.

Block copolymer **A-B2** displays a diffraction pattern consisting of two maxima at $q = 0.47$ and 0.77 nm^{-1}, leading to a peak position ratio of 1.62. This is sufficiently different from the ideal values $\sqrt{2}$, $\sqrt{3}$, or 2, for highly symmetric 2D structures, that their presence can be ruled out. In view of the 2D hexagonal nature of sample **A-B3,** we propose the presence of an oblique 2D packing of cylinders with an angle $\gamma \neq 120°$ and $\gamma \neq 90°$. This causes the six first-order and the six second-order reciprocal lattice points of the 2D hexagonal lattice, which, upon powder average, normally ($\gamma = 120°$) would coincide with the two observed peaks to split up into more or less closely spaced multiplets which can blend into broad peaks that may exhibit characteristic shoulders. For sample **A-B2,** we propose a unit cell with lattice parameters $a = 14.7$ nm, $b = 15.3$ nm, and $\gamma = 111°$ (see Table 2), plane group *P*2 (Col_p). Note that suggesting three lattice constants from two peaks requires the consideration of blended shoulders in the peak shapes and also

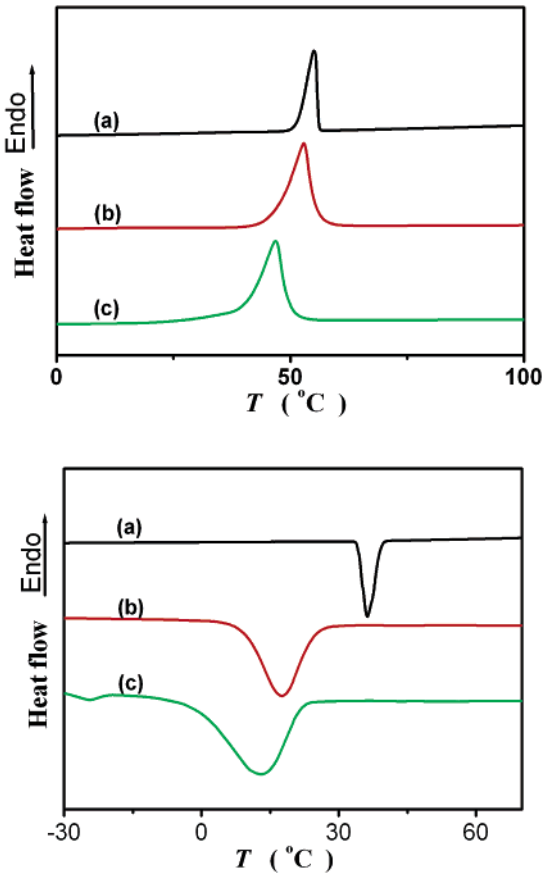

Figure 3. DSC thermograph of second heating flow (left) and cooling flow (right): (a) PEO 2000, (b) **A-B3**, and (c) **A-B2**.

some very low-intensity higher order reflections. The calculated number of **A-B2** molecules in a unit cell is 21.

Thus, a structural change from a *P*2 oblique columnar to a *P*6*mm* hexagonal columnar arrangement with increasing size of monodendron from **A-B2** to **A-B3** was observed in this system. A summary of the diffraction peaks and lattice constants for these extended block copolymers is given in Table 2. According to the molecular architecture of the block copolymers in our system and the data from SAXS profiles, the microdomain structures of **A-B2** and **A-B3** have been presented in Scheme 3.

Crystallization and Crystal Structure of PEO Block. Figure 3 shows the DSC curves of PEO2000 and two block copolymers. The pure PEO sample has a melting temperature $T_m = 55$ °C and the enthalpy of $\Delta H = 171.3$ J/mol, so its degree of crystallization, *x*, is 0.89. Those of **A-B3** and **A-B2** are collected in Table 3. Clearly, they are lower compared to those of the pure PEO samples.

Figure 4 shows the WAXD profiles of the three samples. Two strong Bragg reflections at $2\theta = 18.7°$ and 22.8° show

Table 3. DSC Data of PEO2000, A-B3, and A-B2

	heating		cooling	
	T_m (°C)	ΔH_c (J/mol)[a]	x^b	T_c (°C)
PEO 2000	55.0	171.3	0.89	36.3
A-B3	53.0	127.4	0.65	17.3
A-B2	47.0	96.3	0.49	12.8

[a] Enthalpy for the PEO block, which is calculated by the following equation: $\Delta H/f_v^{PEO}$, where ΔH is the enthalpy from the experimental data for the whole compound and f_v^{PEO} is the volume fractions of PEO. [b] The enthalpy of integrated PEO crystallization is 196 J/mol.

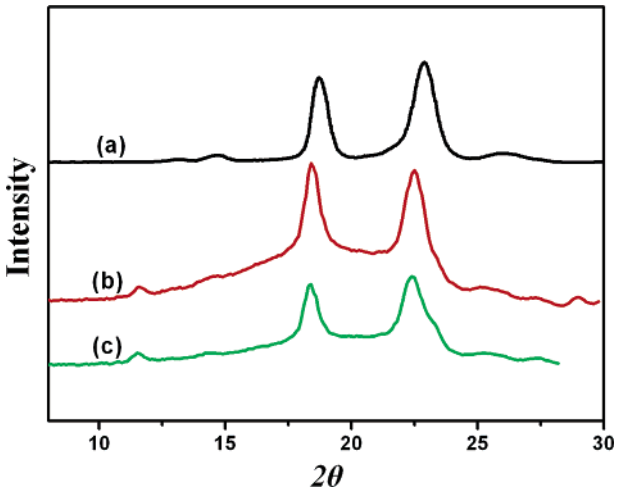

Figure 4. WAXS patterns of (a) PEO 2000, (b) **A-B3**, and (c) **A-B2**.

the monoclinic crystal structure of PEO with a cell parameter of 1.93 nm along the helix axis,[9] further indicating the same structure of PEO crystals in three samples.

Influence of DPA Special Architectures on Curved Interface. The formation of cylindrical microdomains is a consequence of the curved interface, which is always associated with the molecular asymmetry in geometry. In a low molecular mass surfactant system, the formation of supramolecular aggregates depends on the size and geometry of hydrophilic headgroup and hydrophobic tail (see Scheme 4a). A packing parameter,[14] P, defined as $P = V_0/a_e l_0$, which describes the individual molecular geometry as $P \approx 1$ stands for symmetric shape and $P \neq 1$ for asymmetric shape, was recommended to predict the aggregate morphology.[15] The theoretical prediction shows a spontaneous aggregation to form cylinder micelles at $P = 1/3$ to $1/2$. For the linear−linear block copolymers, the microdomain structure depends on the volume fraction of two blocks, f_v, at fixed χN. It is possible to form a curved interface

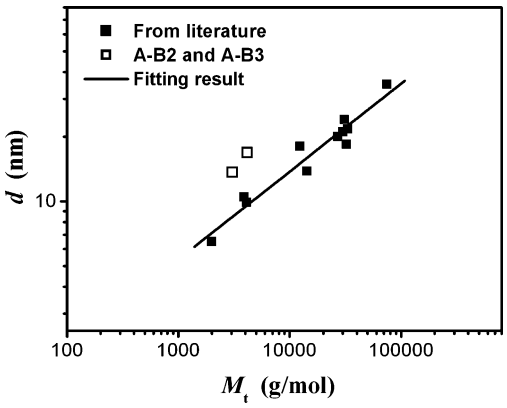

Figure 5. Plot of long period d of cylinder phase against total molecular weight of PEO-containing systems: (solid square) collected from literature;[17] (open square) **A-B3** and **A-B2**.

while $f_v < 0.5$ or $f_v > 0.5$. For A−B block copolymers in the strong segregation regime ($\chi N \geq 100$), a theoretical prediction shows the formation of cylindrical microdomains in the range $0.18 < f_v < 0.4$ or $0.74 < f_v < 0.89$.[16]

For the block copolymers studied, the volume fractions of the PEO blocks in **A-B2** and **A-B3** are 0.61 and 0.41, respectively. Within such a scope of volume fractions, a lamellar structure would normally be expected for conventional linear−linear block copolymer systems instead of a cylindrical structure observed for our system, which also indicates a dominant effect of the molecular architecture over the volume fraction. The fixed conformation of the DPA blocks with wedge-shaped architecture, highly rigid backbone, and persistent structure results in a fixed curvature in the interface between the dendritic and linear blocks, which could conceivably constitute a driving force favoring formation of cylinder in contrast to the lamellar phase formed by their counterpart of linear−linear block copolymers.

Linear−linear block copolymer systems containing PEO as one block have been widely investigated.[17] Figure 5 shows a plot of the long period, d, against the total molecular weight, $\bar{M}_t$, of the PEO-containing block copolymers in which PEO blocks form cylinder microdomain structures. The relation between d and $\bar{M}_t$ obeys a scaling law, $d \propto \bar{M}_t^{\alpha}$, with $\alpha = 0.40 \pm 0.034$ (see solid line). The data of the two hybrid block copolymers are also placed on this figure. Clearly, the total molecular weights of linear−linear PEO-containing block copolymers whose long periods are nearly identical with our system are at least 4 times larger than that of our system. In other words, the cylinder sizes of our hybrid block copolymers are much larger than those of linear−linear block copolymers

Scheme 4. Local Geometry and the Curvature of Domains and Interfaces: (a) Low Molecular Mass Surfactants, (b) Linear−Linear Block Copolymers, and (c) Our Dendritic−Linear Block Copolymer (A-B2)

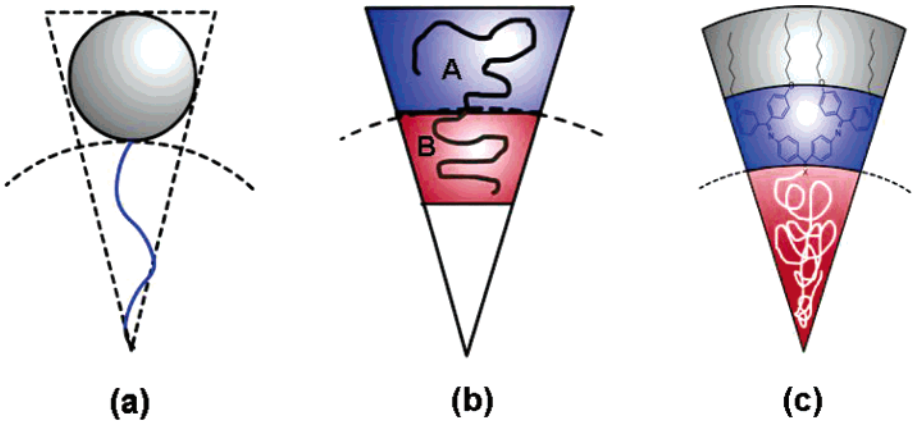

in the same total molecular weight. This further means a construction of somehow "hollow" columns[18] due to the rigid and wedge-shaped architecture of DPA dendrons. This is another way to prove the dominant effect of molecular architecture in DPA dendrons on microdomain structure.

PEO Crystallization in Cylinder Space. The crystallization of the crystallinable block in cylinder or sphere domains can be a confined or unconfined process, depending on the size of the microdomain. The pure PEO2000 forms extended-chain lamellae with a thickness of 12.5 nm (see Figure 2a). From the suggested model presented in Scheme 3, we can calculate the area occupied by PEO blocks in the cylinder aggregates. The estimated diameters for **A-B2** and **A-B3** are 11.6 and 12.4 nm, respectively, which are close to the thickness of extended-chain lamellae of PEO.

The reduction of the melting points and the degree of crystallization of PEO blocks in the two copolymers can be explained by a confined crystallization in the cylinder space (see Scheme S2 in Supporting Information). It is understandable that the thickness of the crystalline PEO phase formed in the hollow columns at the center of DPA coronal should be smaller than the diameters of hollow columns themselves. As a result, the growth of PEO lamellae will be laterally confined in the cylinders to cause the reduction of the melting point and crystallinity of PEO lamellae to a certain extent. On the basis of the relation between melting point and lamellar thickness,[19] the estimated thickness of PEO crystals in the cylindrical space are 8.3 nm for **A-B2** and 12.3 nm for **A-B3**, which are smaller than the diameters of the PEO-occupied area. Note that the estimated diameter of **A-B3** is larger than that of **A-B2**, so the melting point and crystallinity of **A-B2** is reduced more. Finally, it is interesting to mention that the reduction in our copolymers is less than other PEO-containing copolymers[5b] because of the larger cylinder diameter created by the wedge-shaped DPA dendrons. This may indicate that the flexible dendritic blocks with nonconstant conformation backbone cannot hold a large structure as the rigid dendritic blocks does, and therefore, such a conformation-persistent system is more reliable to investigate the detailed process of structure construction.

Conclusion

In summary, we have synthesized two hybrid block copolymers, composed of second- and third-generation dendritic poly(phenylazomethine) (DPA) blocks and a linear PEO block with 2000 g/mol molecular weight. The large molecular asymmetry in architecture and rigidity of the block copolymers make them inclined to form cylindrical microdomain structures which are different from the lamellar structures expected for linear block copolymers of the same volume fraction. Taking the distinctive wedge-shaped DPA blocks into consideration, a somehow "hollow" cylindrical phase is rationalized, as indicated by the unexpectedly large lattice parameters, compared to those of the linear−linear corresponding candidates. Within the cylinders constructed by the DPA dendrons as coronae, the lateral growth of PEO crystal is confined, so as to cause a reduction of the PEO block melting temperature and enthalpy.

Acknowledgment. Financial support given by Nankai University for start-up funding and the National Science Foundation of China for a grant (NSFC20374030) is gratefully acknowledged. We thank Mr. X. X. Duan for assistant of synthesis of the some chemicals used in this work.

Supporting Information Available: Synthesis and structure characterization experimental procedures. This material is available free of charge via the Internet at http://pubs.acs.org.

References and Notes

(1) (a) Noshay, A.; McGrath, J. E. *Block Copolymers, Over View and Critical Survey*; Academic Press: New York, 1977. (b) Hadjichristidis, N.; Paspas, S.; Floudas, G. *Block Copolymers: Synthetic Strategies, Physical Properties, and Application*; John Wiley and Sons: Hoboken, NJ, 2003. (c) Bates, F. S.; Fredrickson, G. H. *Annu. Rev. Phys. Chem.* **1990**, *41*, 525−557; *Annu. Rev. Mater. Sci.* **1996**, *26*, 503−550; *Phys. Today* **1999**, 32−38. (d) Hamley, I. W. *The Physics of Block Copolymers*; Oxford University Press: Oxford, 1998.

(2) (a) Lee, M.; Cho, B. K.; Zin, W. C. *Chem. Rev.* **2001**, *101*, 3869−3892. (b) Klok, H.-A.; Lecommandoux, S. *Adv. Mater.* **2001**, *13*, 1217−1229.

(3) (a) Percec, V.; Johansson, G.; Heck, J.; Ungar, G.; Batty, S. V. *J. Chem. Soc., Perkin Trans. 1* **1993**, 1411−1420. (b) Percec, V.; Cho, W.-D.; Ungar, G.; Yeardley, D. J. P. *J. Am. Chem. Soc.* **2001**, *123*, 1302−1315. (c) Percec, V.; Ahn, C. H.; Ungar, G.; Yeardley, D. J. P.; Möller, M.; Sheiko, S. S. *Nature (London)* **1998**, *391*, 161−164. (d) Percec, V.; Glodde, M.; Bera, T. K.; Miura, Y.; Shiyanovskaya, I.; Singer, K. D.; Balagurusamy, V. S. K.; Heiney, P. A.; Schnell, I.; Rapp, A.; Spiess, H.-W.; Hudson, S. D.; Duan, H. *Nature (London*) **2002**, *419*, 384−387. (e) Ungar, G.; Liu, Y. S.; Zeng, X. B.; Percec, V.; Cho, W. D. *Science* **2003**, *299*, 1208−1211. (f) Zeng, X. B.; Ungar, G.; Liu, Y. S.; Percec, V.; Dulcey, S. E.; Hobbs, J. K. *Nature (London)* **2004**, *428*, 157−160.

(4) (a) Gitsov, I.; Wooley, K. L.; Fréchet, J. M. J. *Angew. Chem., Int. Ed.* **1992**, *31*, 1200−1202. (b) Gitsov, I.; Ivanova, P. T.; Fréchet, J. M. J. *Macromol. Rapid Commun.* **1994**, *15*, 387−393. (c) Chapman, T. M.; Hillyer, G. L.; Mahan, E. J.; Schaffer, K. A. *J. Am. Chem. Soc.* **1994**, *116*, 11195−11196. (d) Gitsov, I.; Fréchet, J. M. J. *J. Am. Chem. Soc.* **1996**, *118*, 3785−3786. (e) Leduc, M. R.; Hawker, C. J.; Dao, J.; Fréchet, J. M. J. *J. Am. Chem. Soc.*. **1996**, *118*, 11111−11118. (f) Hest, J. C. M. v.; Delnoye, D. A. P.; Baars, M. W. P. L.; Elissen-Román, C.; Genderen, M. H. P. V.; Meijer, E. W. *Chem.—Eur. J.* **1996**, *2*, 1616−1626. (g) Iyer, J.; Fleming, K.; Hammond, P. T. *Macromolecules* **1998**, *31*, 8757−8765. (h) Chang, Y.; Kwon, Y. C.; Lee, S. C.; Kim, C. *Macromolecules* **2000**, *33*, 4496−4500. (i) Lambrych, K. R.; Gitsov, I. *Macromolecules* **2003**, *36*, 1068−1074. (j) Lecommandoux, S.; Klok, H.-A.; Sayar, M.; Stupp, S. I. *J. Polym. Sci., Polym. Chem.* **2003**, *41*, 3501−3518.

(5) (a) Gitsov, I.; Wooley, K. L.; Hawker, C. J.; Ivanova, P. T.; Fréchet, J. M. J. *Macromolecules* **1993**, *26*, 5621−5627. (b) Cho, B. K.; Jain, A.; Gruner, S. M.; Wiesner, U. *Chem. Commun.* **2005**, 2143−2145. (c) van Hest, J. C. M.; Delnoye, D. A. P.; Baars, M. W. P. L.; van Genderen, M. H. P.; Meijer, E. W. *Science* **1995**, *268*, 1592−1595. (d) van Hest, J. C. M.; Baars, M. W. P. L.; Elissen-Román, C.; Genderen, M. H. P. V.; Meijer, E. W. *Macromolecules* **1995**, *28*, 6689−6691. (e) Mackay, M. E.; Hong, Y.; Jeong, M.; Tande, B. M.; Wagner, N. J.; Hong, S.; Gido, S. P.; Vestberg, R.; Hawker, C. J. *Macromolecules* **2002**, *35*, 8391−8399. (f) Pochan, D. J.; Pakstis, L.; Huang, E.; Hawker, C. J.; Vestberg, R.; Pople, J. *Macromolecules* **2002**, *35*, 9239−9242. (g) Gitsov, I.; Fréchet, J. M. J. *Macromolecules* **1993**, *26*, 6536−6546. (h) Duan, X. X.; Yuan, F.; Wen, X. J.; Yang, M.; He, B. L.; Wang, W. *Macromol. Chem. Phys.* **2004**, *205*, 1410−1417. (i) Pickett, G. T. *Macromolecules* **2002**, *35*, 1896−1904. (j) Zubarev, E. R.; Sone, E. D.; Stupp, S. I. *Chem.-Eur. J.* **2006**, *12*, 7313−7327.

(6) Grason, G. M. *Phys. Rep.* **2006**, *433*, 1−64.

(7) Miyaura, N.; Suzuki, A. *Chem. Rev.* **1995**, *95*, 2457- 2483.

(8) (a) Higuchi, M.; Shiki, S.; Yamamoto, K. *Org. Lett.* **2000**, *2*, 3079−3082. (b) Higuchi, M.; Shiki, S.; Ariga, K.; Yamamoto, K. *J. Am. Chem. Soc.* **2001**, *123*, 4414−4420.

(9) Takahashi, Y.; Tadokoro, H. *Macromolecules* **1973**, *6*, 672- 675.

(10) Immirzi, A.; Perini, B. *Acta Crystallogr.* **1977**, *A33*, 216−218.

(11) (a) Oriz, W.; Roitberg, A. E.; Krause, J. L. *J. Phys. Chem. B* **2004**, *108*, 8218−8225. (b) Han, M.; Chen, P.; Yang, X. *Polymer* **2005**, *46*, 3481−3488. (c) Maiti, P. K.; Craig, T.; Wang, G.; Goddard III, W. A. *Macromolecules* **2004**, *37*, 6236−6254. (d) Boris, D.; Rubinstein, M. *Macromolecules* **1996**, *29*, 7251−7260. (e) Chai, M.; Niu, Y.; Youngs, W. J.; Rinaldi, P. L. *J. Am. Chem. Soc.* **2001**, *123*, 4670−4678. (f) Potschke, D.; Ballauff, M.; Lindner, P.; Fischer, M.; Vogtle, F. *Macromolecules* **1999**, *32*, 4079−4087. (g) Ballauff, M. *Top. Curr. Chem.* **2001**, *212*, 177−194.

(12) Kollbel, M.; Beyersdorff, T.; Cheng, X. H.; Tschierske, C.; Kain, J.; Diele, S. *J. Am. Chem. Soc.* **2001**, *123*, 6809−6818.

(13) (a) Satoh, N.; Cho, J. S.; Higuchi, M.; Yamamoto, K. *J. Am. Chem. Soc.* **2003**, *125*, 8104−8105. (b) Imaoka, T.; Tanaka, R.; Arimoto, S.; Sakai, M.; Fujii, M.; Yamamoto, K. *J. Am. Chem. Soc.* **2005**,

127, 13896−13905. (c) Higuchi, M.; Shiki, S.; Ariga, K.; Yamamoto, K. *J. Am. Chem. Soc.* **2001**, *123*, 4414−4420.
(14) Isrealachvili, J. N.; Mitchell, D. J.; Ninham, B. W. *J. Chem. Soc., Faraday Trans. 2* **1976**, *72*, 1525−1568.
(15) Föster, S.; Plantenburge, T. *Angew. Chem., Int. Ed.* **2002**, *41*, 688−714.
(16) Reference 1d, p 73.
(17) (a) Huang, P.; Guo, Y.; Quirk, R. P.; Ruan, J.; Lotz, B.; Thomas, E. L.; Hsiao, B. S.; Avila-Orta, C. A.; Sics, I.; Cheng, S. Z. D. *Polymer* **2006**, *47*, 5457−5466. (b) Sun, L.; Zhu, L.; Ge, Q.; Quirk, R. P.; Xue, C. C.; Cheng, S. Z. D. *Polymer* **2004**, *45*, 2931−2939. (c) Evans, C. C.; Bates, F. S.; Ward, M. D. *Chem. Mater.* **2000**, *12*, 236−249. (d) Hamersky, M. W.; Hillmyer, M. A.; Tirrell, M.; Bates, F. S.; Lodge, T. P.; von Meerwall, E. D. *Macromolecules* **1998**, *31*, 5363−5370. (e) Gervais, M.; Gallot, B. *Makromol. Chem.* **1973**, *171*, 157−178. (f) Gervais, M.; Gallot, B. *Makromol. Chem.* **1973**, *174*, 193−214.
(18) Percec, V.; Holerca, M. N.; Nummelin, S.; Morrison, J. J. *Chem.—Eur. J.* **2006**, *12*, 6216−6241.
(19) Cheng, S. Z. D.; Chen, J.; Janimak, J. J. *Polymer* **1990**, *31*, 1018.

MA062881L